Original Article

Histological Evaluation of the Possible Ameliorative Effect of SGLT2 Inhibitor versus ACE Inhibitor on Podocytes Following Unilateral Nephrectomy in Young Male Albino Rats

Mariam Ezzat Helmy, Dalia Fathy El- Deeb, Eman Abas Farag and Samia Hamdy Radwan

Department of Histology, Faculty of Medicine, Cairo University, Cairo, Egypt

ABSTRACT

Background: The compensatory changes following renal mass reduction are harmful to the remaining kidney tissue in the long run. Therefore, they have to be controlled early. The current study aimed to detect the histological changes in podocytes following unilateral nephrectomy in young male albino rats, and to evaluate the possible ameliorative effect of sodium glucose cotransporter 2 inhibitor (SGLT2I) versus angiotensin converting enzyme inhibitor (ACEI) by histological and morphometric studies.

In this study, 48 young male albino rats were used; 6 control rats (group I), 6 sham operated (group II), and the remaining 36 were subjected to uninephrectomy, then randomly equally divided into 3 groups: (group III) was left untreated, (group IV) received an ACEI [enalapril], and (group V) received an SGLT2I [dapagliflozin]. The drugs were given daily for 2 weeks. Before sacrifice, the rats were subjected to serum creatinine and 24-hour urinary albumin measurements. After sacrifice, histological and immunohistochemical analysis for nestin were done. Transmission electron microscopy (TEM) was used to examine the ultrastructural changes in podocytes and to measure the glomerular basement membrane (GBM) thickness.

Morphometric studies were done to measure Bowman's space and glomerular areas, and area percent of nestin immune reactivity. All measurements were statistically analyzed.

Results: The histological outcome that followed uninephrectomy in the untreated group showed all the criteria of focal segmental glomerulosclerosis (FSGS). This outcome was ameliorated by the early administration of the ACEI and SGLT2I. Both treated groups showed significant reduction in Bowman's space area, area percent of nestin, and GBM thickness when compared to the untreated group. However, no significant difference could be detected between the two treated groups denoting the drugs' almost similar efficacy.

Conclusion: SGLT2I is almost equally effective as the ACEI. Therefore, it could be given following renal mass reduction whenever the ACEI is contraindicated, untolerated, or inadequate.

Received: 12 August 2023, **Accepted:** 02 October 2023

Key Words: ACEI; FSGS; podocyte; SGLT2I; unilateral nephrectomy.

Corresponding Author: Mariam Ezzat Helmy, MSc, Department of Histology, Faculty of Medicine, Cairo University, Cairo, Egypt, **Tel.**: +20 12 2271 2895, **E-mail:** to_mariam@cu.edu.eg

ISSN: 1110-0559, Vol. 47, No. 4

BACKGROUND

Podocytes are highly differentiated epithelial cells that share in the glomerular filtration barrier formation[1]. These precious unique cells are exposed to several mechanical stresses such as the glomerular capillary pressure and the glomerular filtration[2]. These stresses intensify following renal mass reduction, resulting in glomerular hypertension which creates tensile stress on the foot processes, and hyperfiltration which creates fluid flow shear stress (FFSS) on the cell body and major processes of podocytes. Continuous mechanical stresses might result in damage and loss of podocytes, which affect the integrity of the filtration barrier resulting in progressive renal disease[3].

Unilateral nephrectomy is one of the causes of renal mass reduction, in which there is loss of half the number of functioning nephrons. This surgical procedure is an essential step in living kidney donation, that might result in end stage renal disease (ESRD) for the donor and a need for replacement therapy on the long run as a result of hyperfiltration[4]. It is worth mentioning that the first living donor, Ronald Lee Herrick, in 1954, spent the last 10 years of his life on dialysis[5]. Therefore, treatments for chronic kidney disease (CKD) should be targeting the protection of podocytes from injury[6].

The inhibition of the renin- angiotensin- aldosterone system (RAAS) is one of the well-known therapies used to manage CKD. However, in some conditions further treatments may be essential[7], due to drug intolerance or suboptimal dosing to evade common side effects of RAAS blockers such as hyperkalemia[8]. SGLT2Is are a new class of antidiabetic drugs[9], that were found to diminish the risk of renal events as proved by multiple large clinical trials[10], therefore, it was justified to try them in renal non-diabetic models[11]. In 2021, the US Food and Drug Administration (FDA) approved dapagliflozin for use in cases of CKD

DOI: 10.21608/ejh.2023.228422.1933

irrespective of the diabetic status[12,13]. However, the FDA did not mention its use in cases of solitary kidney in specific. Therefore, the benefit of SGLT2Is for renal non-diabetic models with different varieties of CKD is still under investigation[14].

Research should be directed to understand exactly all the mechanical forces affecting podocytes, targeting to identify new treatments that would complement or replace the currently used RAAS blockers in controlling renal diseases[5]. Thus, the current study aimed to detect the histological changes in podocytes following unilateral nephrectomy in young male albino rats, and to evaluate the possible ameliorative effect of SGLT2I versus ACEI by histological and morphometric studies.

MATERIALS AND METHODS

Drugs

Ezapril (enalapril maleate): It is an ACEI provided by Apex Pharma, Egypt. It is available in the form of tablets (each contains 10 mg).

Forxiga (dapagliflozin): It is an SGLT2I provided by AstraZeneca, UK. It is available in the form of tablets (each contains 10 mg).

Each drug was crushed into powder and added to distilled water to be given by orogastric gavage.

Experimental animals

Forty-eight male albino rats at 1 month age (~50- 60 gm weight) were included in this study. Rats were provided and given veterinary care by the Animal house of Kasr Al-Ainy, Faculty of Medicine, Cairo University. They were caged at room temperature with 12-h light-dark cycles and free access to standard food and water for one week for acclimatization. All experimental protocols were approved by the animal ethical committee of Faculty of Medicine, Cairo University (approval number CUIIIF1622).

Rats were randomly divided into the following groups:

Control group (Group I): Six rats were included in this group.

Sham operated group (Group II): Six rats were sham operated by left kidney manipulation without ligation of the renal vessels or the ureter.

The rest of the rats underwent unilateral nephrectomy and were randomly divided into 3 groups, 12 rats each.

Untreated unilateral nephrectomy group (Group III): Twelve uninephrectomized rats were left untreated.

Rats from groups I, II, and III were given 0.5 ml of distilled water by orogastric gavage once daily until the time of sacrifice.

ACEI treated group (Group IV): Twelve uninephrectomized rats were given ezapril by orogastric gavage once daily starting postoperative and until the time of sacrifice, at a dose of 10 mg/kg/ day[15]. Accordingly, 0.5 mg/day/rat was given as a starting dose (each rat received 0.5 ml of the drug suspension containing the daily required dose).

SGLT2I treated group (Group V): Twelve uninephrectomized rats were given forxiga by orogastric gavage once daily starting postoperative and until the time of sacrifice, at a dose of 1.5 mg/kg/ day[11]. Accordingly, ~ 0.08 mg/day/rat was given as a starting dose (each rat received 0.5 ml of the drug suspension containing the daily required dose).

Drug suspensions were given after very well shaking to assure proper dosage, which was adjusted according to weight gain (It was checked every 2 days) during the experimental period.

All rats were sacrificed 2 weeks following sham operation and unilateral nephrectomy.

Experimental procedures

Unilateral nephrectomy: Animals were anesthetized using Ketamine and Xylazine combination (Ketamine 90 mg/kg; Xylazine 10 mg/kg body weight intraperitoneal)[16]. Rat's abdominal skin was shaved and disinfected prior to surgery using chlorhexidine in combination with alcohol[17]. A midline incision extending from the xiphoid process to the infraumbilical region was made. The abdominal muscles were retracted to explore the abdominal contents till the left kidney was reached. Its blood supply was identified, isolated and ligated few millimeters away from the renal hilum. The renal vessels with their accompanying ureter were then incised. After that, the left kidney was dissected out from the retroperitoneal space[18].

Following the aforementioned actions, the abdominal contents were gently returned to their anatomical positions. The abdominal muscles and the skin were sutured in layers with sterile 3-0 chromic gut sutures and 3-0 Ethilon monofilament nylon suture and cutting needle. Further to this, each rat was gently placed in a recovery cage with free access to food and water ad libitum[18]. In addition, care of the wound was done by spraying the topical antibiotic Bivatracin (Neomycin sulphate 165,000 IU + Bacitracin zinc 12,500 IU - provided by ACDIMA international trading company) on the sutured area once daily for 3 days starting from the day of the operation[19]. The animals were transferred to their usual cages following recovery and until sacrifice.

Sham operation: For the sham operated rats, the same steps as in unilateral nephrectomy were taken, with only manipulation of the left kidney.

Laboratory studies: Blood and urine samples were collected from all experimental rats before sacrifice.

Each rat had the following tests

Serum creatinine: tail vein blood samples were collected from each rat using a 22 G butterfly needle and analyzed for serum creatinine.

24-hour urinary albumin: each rat was placed separately in a "metabolic cage", with free access for food and water, to collect urine in 24 hours.

The lab. investigations were measured in the "Immune Measurement and Hormones Analyses Lab", Faculty of Agriculture, Cairo University. The temperature and relative humidity of the environment during the analysis were 25.6°C and 42.5% respectively.

For creatinine analysis

Spectrum: Kinetic Jaffe Method- Creatinine Assay- Cat No:234001.

Test method: TM-Creatinine- 01.01/ Spectrophotometer.

For 24-hour urinary albumin

Spectrum: Colorimetric Method- Albumin Assay- Cat No:211001.

Test method: TM-Albumin- 01.01/ Spectrophotometer.

Each albumin value was then multiplied by the volume of urine of its sample (to calculate its amount in 24-hour).

Euthanasia

Two weeks following sham operation and unilateral nephrectomy- the average weight of the rats was 100-120 gm- all rats were euthanized at the Laboratory Animal House Unit by humane cervical dislocation under anesthesia by intraperitoneal injection of pentobarbital at a dose of 50 mg/kg body weight[20]. According to a previous study[21], it is the best sacrifice method for histological and histopathological studies of the kidney. The immediate dislocation of the atlantoaxial joint (confirmed by a crack sound) ensured sudden death in few seconds, followed by removal of the rats' right-sided kidneys. The weight of each collected kidney was recorded.

Histological procedures

For light-microscopic examination

Slides were prepared and examined in the Histology Department, Cairo University.

Right kidney specimens (parts that remained after cutting blocks for EM) were fixed in 10% buffered formalin solution for 24 hours, dehydrated in ascending grades of ethanol and embedded in paraffin wax. Serial transverse sections were cut at 7 µm thickness, mounted on glass slides, and stained with:

1. Hematoxylin and Eosin stain (H&E)[22].
2. Immunohistochemical staining for the intermediate filament nestin:

Nestin rabbit Ig/G polyclonal antibody (Thermo scientific, Corporation laboratories), Catalogue Number: PA5-79729, available in a concentrated liquid form (500 µg/ml) that was diluted at 0.5-1 µg/ml. It's a marker for the intermediate filament nestin that appears as a brown cytoplasmic reaction in podocytes[23].

Immunostaining using avidin–biotin technique required pretreat[22]. The sections were boiled for 10 min in 10 mM citrate buffer (cat no 005000) pH 6 for antigen retrieval. Then, they were put to cool for 20 min at room temperature. Following, the sections were incubated with the primary antibodies for 1 hour. Immunostaining was accomplished using Histostain SP kit (LAB-SA system, Zymed Laboratories Inc, San Francisco, CA 94080, USA, catalogue number 95-9643), which is a broad-spectrum detection system that reacts with mouse, rabbit, guinea pig, and rat primary antibodies. Negative control kidney sections were prepared by the same process but with skipping the step of adding primary antibody. Counterstaining using Lab Vision Mayer's hematoxylin (cat no TA- 060- MH) was accomplished.

3- Semithin sections[22]

Approximately 3-mm3 cortical tissue blocks from the right kidneys were fixed by immersion in 2.5% glutaraldehyde in phosphate buffered saline (PBS) (0.1 mol/L, pH 7.2), postfixed in 1% osmium tetroxide in PBS (0.1 mol/L, pH 7.2), dehydrated in a graded series of ethanol, embedded in Fluka Epon 812 resin (Sigma-Aldrich Chemica, Steinheim, Switzerland), and polymerized at 60C. The Epon blocks were sectioned with glass knives on a microtome (Ultracut R; Leica, Wien, Austria).

Semithin sections were prepared on glass slides through cutting at 1um using the ultra-microtome. Sections were stained with toluidine blue for 25 seconds and examined by light microscope in order to locate and trim the areas chosen for TEM studying.

For TEM evaluation

Ultrathin sections were cut at 60 nm, collected on 200-mesh naked copper grids and stained with uranyl acetate and lead citrate[22]. This work was done in the TEM laboratory at Cairo University Research Park (CURP)- Faculty of Agriculture. Ultra-thin tissue sections were examined by transmission electron microscope JEOL (JEM-1400 TEM) at different magnifications. Images were captured by CCD camera model AMT with 1632 × 1632-pixel format as side mount configuration. This camera uses 1394 firewire board for acquisition.

Morphometric studies

Measurements were done using "Leica Qwin 500 C" image analyzer computer system Ltd. (Cambridge, England) at the Histology Department, Faculty of Medicine, Cairo University. The following parameters were measured in ten non overlapping fields for each animal in each group:

- Bowman's space area in H&E-stained paraffin sections (at ×100 magnification).
- Glomerular area in H&E-stained paraffin sections (at ×100 magnification).
- Area % of positive nestin immune expression (at ×400 magnification).

GBM thickness: It was measured during ultrathin sections' examination by TEM (Figure 1 a-d), between the basal part of the endothelial membrane and the basal part of the podocyte membrane that touches the GBM[24].

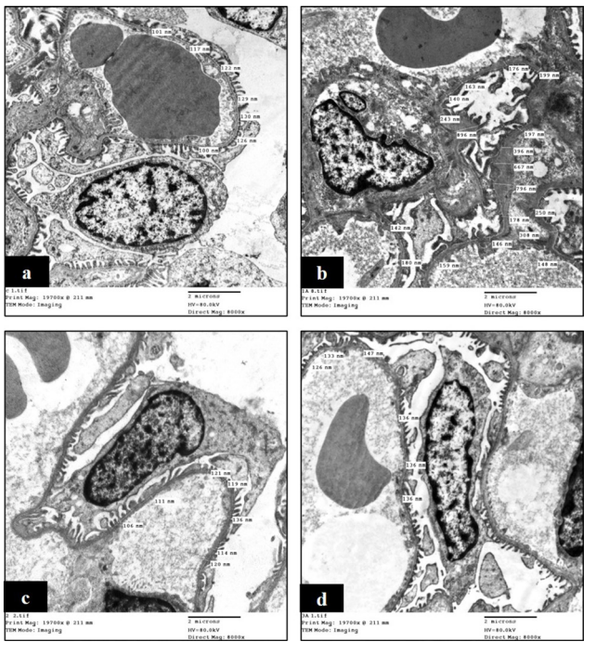

Fig. 1: [a, b, c &d]: Electron micrographs from groups I, III, IV&V, respectively, on which GBM thickness is measured at several points (TEM X 8000).

Statistical analysis

The obtained measurements were statistically analyzed using IBM SPSS® statistics version 26 (IBM® Corporation, Armonk, NY, USA). Numerical data were expressed as mean, standard deviation and range. Data were tested for normality using Kolmogorov-Smirnov test and Shapiro-Wilk test. Data were found to be normally distributed so comparison between more than two groups was done using analysis of variance (ANOVA), then post-Hoc test "Tukey HSD" was used for pair-wise comparison. All tests were two-tailed. A *p-value* less than or equals 0.05 was considered significant

RESULTS

General Observations

Mortality

Three rats died during the experimental period; one from group IV (ACEI treated group) at day 4, and two from group V (SGLT2I treated group) at day 6.

Kidney weight in grams at time of sacrifice: (Figure 2a)

The average kidney weight revealed a non-significant difference between the control and sham operated groups (*p-value* 1). In comparison to the control, the average kidney weight showed significant increase (*p- value* < 0.05) in groups III, IV and V, with no significant difference between the three experimental groups.

Biochemical Results

Serum creatinine expressed in mg/dl: (Figure 2b) & 24-hour urinary albumin expressed in mg/day: (Figure 2c)

The average serum creatinine as well as the 24-hour urinary albumin showed no significant difference between the control and sham operated groups (*p-value* 0.99). In comparison to the control, these measurements didn't show any increase in the uninephrectomized rats (*p-value*~1) with no significant difference between the three experimental groups (*p- value* ~1).

Histological Results

In all histological and statistical studies done, sham operated rats showed similar results as control. Accordingly, only photomicrographs from the control group were included.

Control group (group I): H&E-stained sections of the cortex of right kidneys (Figure 3 a,b) showed normal renal histoarchitecture, particularly the glomerulus and Bowman's space (which are the scope of this study). The flat epithelial cells lining Bowman's capsule could be identified in the photomicrographs. Within the capsule, the glomerular tuft appeared normal and was separated from Bowman's capsule by Bowman's space.

Nestin immune-stained sections demonstrated positive cytoplasmic expression in podocytes, parietal layer of Bowman's capsule, and glomerular endothelial cells (Figure 3c).

The ultra-thin sections of renal cortex from this group (Figure 3 d-g) showed normal glomerular ultrastructure in which podocytes were surrounding the glomerular capillary loops. Their cytoplasm contained rough endoplasmic reticulum (rER), ribosomes and Golgi apparatus. Bundles of microtubules could be seen within the major processes in some of the micrographs. In addition, foot processes were resting on a GBM of uniform thickness, and separated from each other by slit diaphragms. Normally appearing subpodocytic space was noted in control rats. Mesangial areas were identified containing mesangial cells surrounded by mesangial matrix.

Untreated unilateral nephrectomy group (group III): H&E-stained sections (Figure 4 a-d) revealed distortion of some glomeruli. Others showed increased extracellular matrix leading to obliteration of some glomerular capillary loops in some areas of the tuft. This pathology was found only in some glomeruli and in some capillary loops, not the whole tuft. Widening of Bowman's space was detected in most of the glomeruli. While in some others, obliteration of Bowman's space could be noticed, with frequent adhesions between the tuft of capillaries and the parietal layer of Bowman's capsule. Furthermore, some glomeruli expressed the homogenous eosinophilic material of hyaline deposits (hyalinosis).

Nestin immune-stained sections showed intense cytoplasmic expression of nestin in podocytes and the

parietal layer of Bowman's capsule. Nestin positive podocytes crossed Bowman's space and came in contact with the parietal epithelial cells (Figure 4e).

Ultra-structurally (Figure 5 a-g), renal cortex from untreated uninephrectomized rats showed altered ultrastructure in which some podocytes had heterochromatic or even pyknotic nuclei. Some of them exhibited vacuolations and endocytic vesicles. Microvillus transformation and cytoplasmic shedding were detected. Moreover, foot processes appeared distorted, and they displayed areas of effacement. Furthermore, in some micrographs, foot processes disappeared in limited areas where the GBM was covered directly by the major processes of podocytes, while in some other locations the GBM was directly covered by the cell body itself. Adhesions between podocytes and the parietal layer of Bowman's capsule, and between podocytes themselves could also be noticed. Occasionally, podocytes were separated and floating in Bowman's space, however they appeared viable with intact foot processes. Subpodocytic space appeared widened in these rats. GBM presented areas of localized thickening which sometimes resembled mushroom-like projections. Lastly, mesangial expansion was observed.

ACEI treated group (Group IV): H&E-stained sections (Figure 6 a,b) verified marked preservation of the renal histoarchitecture, in which the glomeruli appeared normal without distortion or adhesions. However, some capillaries showed mild congestion with dilatation. The glomerular tufts were surrounded by seemingly normal Bowman's spaces.

Nestin immune-stained sections showed weak positive cytoplasmic expression in podocytes and the parietal layer of Bowman's capsule (Figure 6c).

Ultra-structurally (Figure 6: d-f), the renal cortex showed marvelous preservation of the glomerular ultrastructure in which podocytes contained Golgi apparatus, rER, and very few small vacuolations in their cytoplasm. In addition, foot process effacement was infrequently encountered. Foot processes were resting on a GBM of uniform thickness. Subpodocytic space appeared normal in these rats.

SGLT2I treated group (Group V): H&E-stained sections (Figure 7 a,b) showed obvious histoarchitectural preservation in the renal cortex, particularly the glomeruli and Bowman's spaces which appeared normal surrounding glomerular tufts of capillaries.

Nestin immune-stained sections revealed weak cytoplasmic expression of nestin in podocytes (Figure 7c).

Ultra-structurally (Figure 7 d-f), the renal cortex showed marked preservation of the glomerular ultrastructure in which podocytes contained rER and ribosomes, with occasionally detected vacuolations in their cytoplasm. In addition, foot processes kept their characteristic shape in most of the fields. They were resting on a GBM of uniform thickness, and separated from each other by slit diaphragms. However, few areas of foot process effacement were detected. Subpodocytic space appeared normal in these rats.

Morphometric and Statistical Results

Bowman's space area expressed in µm²

The average area of Bowman's space in the control and sham operated groups revealed no significant difference between them (*p-value* 1). In comparison to the control, the average Bowman's space area was increased in all experimental groups, showing a significant rise in group III (*p- value* <0.001) and in group IV (*p- value* 0.006). However, the increase in Bowman's space area was not significant in group V (*p- value* 0.1). Groups IV and V showed significant reduction in Bowman's space area (*p- value* <0.001) when compared to group III. Meanwhile, there was no significant difference (*p- value* 0.98) between both groups when compared to each other (Figure 8a).

Glomerular area expressed in µm²

The average glomerular area in the control and sham operated groups demonstrated no significant difference between them (*p-value* 1). In comparison to the control, the average glomerular area showed a significant rise in group III (*p- value* <0.05) and group IV (p- value 0.05). However, it did not increase in group V (*p- value* 1).

When compared to group III, group IV didn't show any significant difference in glomerular area (*p- value* 0.99), unlike group V which showed a significant reduction in glomerular area (*p- value* 0.05). The difference in the glomerular area between groups IV and V was insignificant (*p- value* 0.08) (Figure 8b).

Area % of positive immune reaction of nestin

The average area % of nestin in the control and sham operated groups showed no significant difference between them (*p-value* 0.99). Compared to the control, the average area % of nestin showed a significant rise in group III (*p- value* <0.001). However, it did not increase in groups IV & V (*p- value* ~1). When compared to group III, groups IV and V showed significant reduction in the average area % of nestin (*p- value* <0.001), while the difference between both groups was insignificant (*p- value* 1) (Figure 8c).

GBM thickness expressed in nm

The average GBM thickness in the control and sham operated groups demonstrated no significant difference between them (*p-value* 1). In comparison to the control, the average GBM thickness showed a significant rise in group III (*p- value* <0.001). However, it did not increase in group IV (*p- value* 0.98), or in group V (*p- value* 0.99). When compared to group III, groups IV and V showed significant reduction in GBM thickness (*p- value* <0.001). The difference between both groups was insignificant (*p- value* 0.89) (Figure 8d).

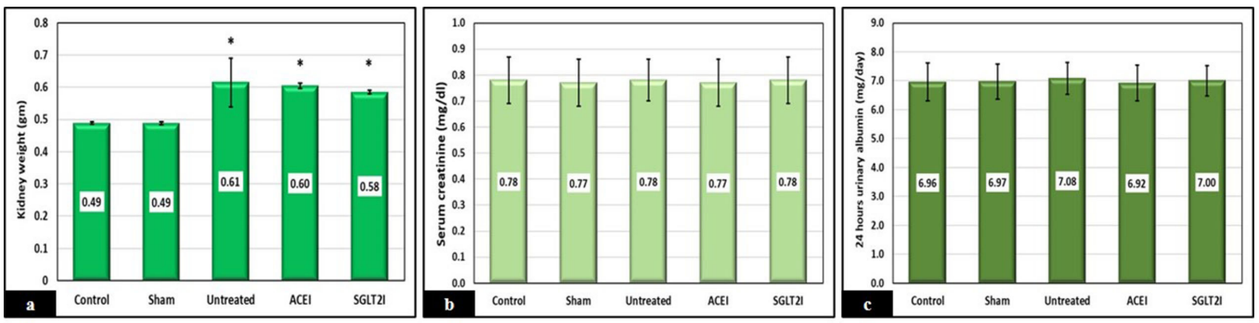

Fig. 2: Histograms showing the mean values ± SD of: **[a]:** kidney weight in the studied groups at time of sacrifice expressed in grams. *Significant increase as compared to control (*p-value* ≤ 0.001) **[b]:** serum creatinine expressed in mg/dl. **[c]:** 24-hour urinary albumin expressed in mg/day.

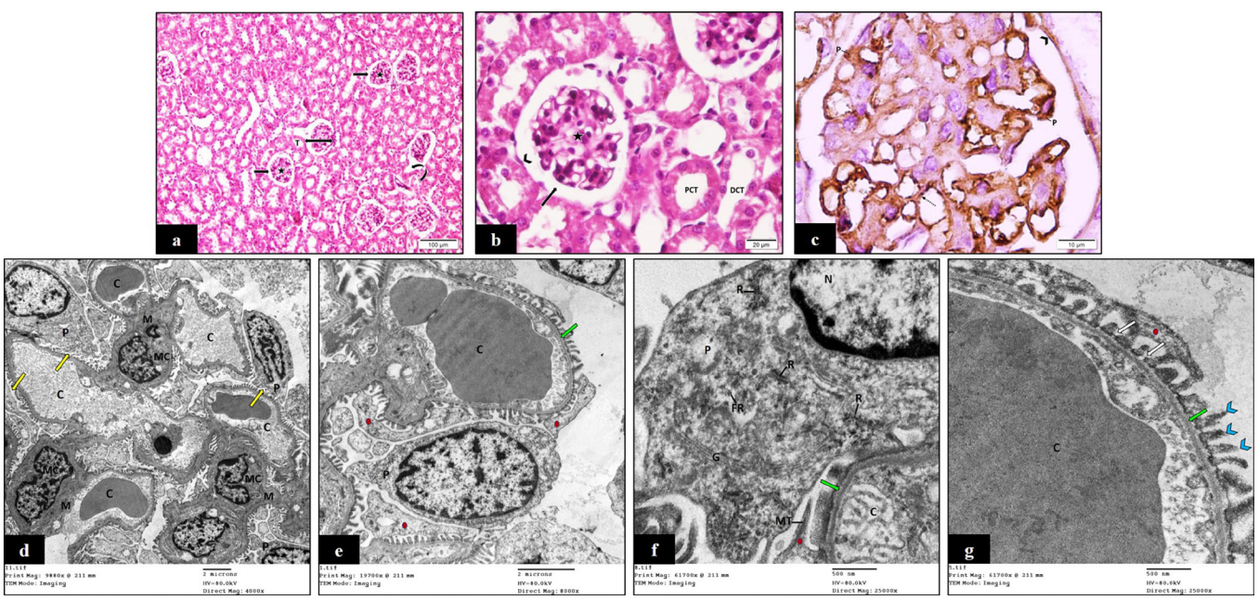

Fig. 3: Photomicrographs of the renal cortex from control group (group I):
[a&b]: normally appearing renal corpuscles (double headed arrow) present among renal tubules (T), which are proximal (PCT) and distal convoluted tubules (DCT). Each glomerular tuft of capillaries (star) is separated from the parietal epithelial lining of Bowman's capsule (arrow head) by Bowman's space (arrow). Note the tubular pole is seen in some corpuscles (curved arrow). [a: H&E, x100, b: H&E, x400]. [c]: positive cytoplasmic immune reactivity of nestin in podocytes (P), parietal layer of Bowman's capsule (arrow head) and glomerular endothelial cells (dotted line arrow). [anti nestin immunohistochemical stain, x1000]. [d]: part of a glomerulus in which podocytes (P) can be seen surrounding glomerular capillary loops (C), with normally appearing subpodocytic spaces (yellow arrows). The mesangial areas show mesangial cells (MC) surrounded by mesangial matrix (M). [TEM, x4000]. [e]: showing a podocyte (P), major processes (red dots), and a glomerular capillary loop (C). GBM appears regular and of a uniform thickness (Green arrow). [TEM, x8000]. [f]: showing the cell body of one podocyte (P) occupying most of the field, a glomerular capillary loop (C), and GBM (green arrow). The podocyte shows an euchromatic nucleus (N), rER (R), free ribosomes (FR) and Golgi apparatus (G). Bundles of microtubules (MT) can be visualized within the major process (red dot). [TEM, x25000]. [g]: part of a glomerular capillary loop (C), a major process (red dot), foot processes (blue arrow heads) and slit diaphragms (white arrows) are seen. GBM (green arrow) has a regular thickness. [TEM, x25000].

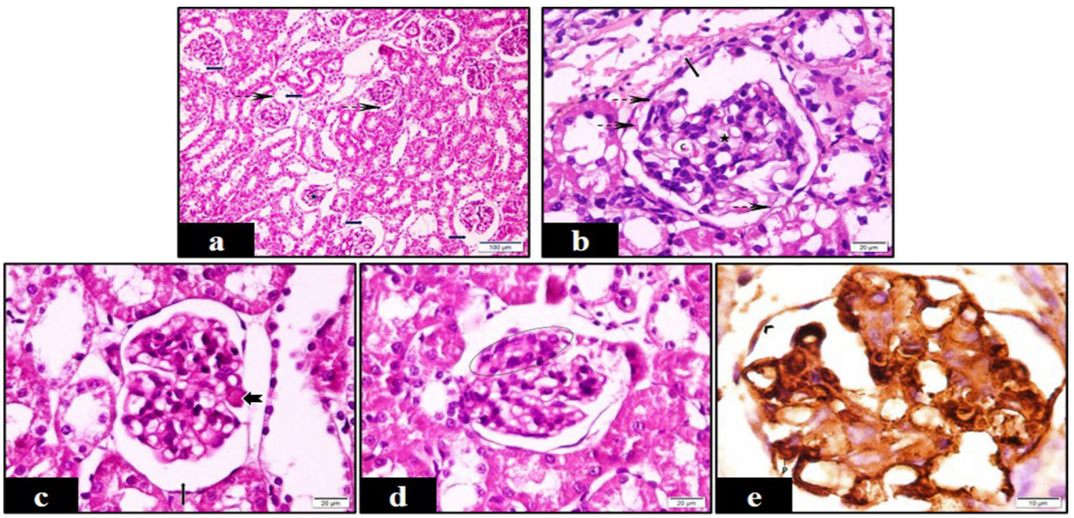

Fig. 4: Photomicrographs of the renal cortex from untreated unilateral nephrectomy group (group III):
[a]: showing some distorted glomeruli (star) with dilated Bowman's spaces (arrows). Adhesions between the glomerular tufts and the parietal layer of Bowman's capsule can be seen (dashed arrows). [H&E, x100]. [b]: a distorted glomerulus (star), widened Bowman's space (arrow), and adhesions between the tuft and the parietal epithelium are noticed (dashed arrows). Note glomerular capillaries show dilatation (C). [H&E, x400]. [c]: demonstrating enlarged renal corpuscle with widened Bowman's space (arrow). An area of homogenous eosinophilic material (hyaline deposits) can be seen in the vascular pole area (notched arrow). [H&E, x400]. [d]: The glomerulus shows increased extra cellular matrix with obliteration of glomerular capillary loops in a segment of the tuft (oval outline). [H&E, x400]. [e]: intense cytoplasmic expression of nestin in podocytes (P) is seen, which crossed Bowman's space and became in contact with the parietal epithelial cells. The later also show positive expression of nestin (arrow head). [anti nestin immunohistochemical stain, x1000].

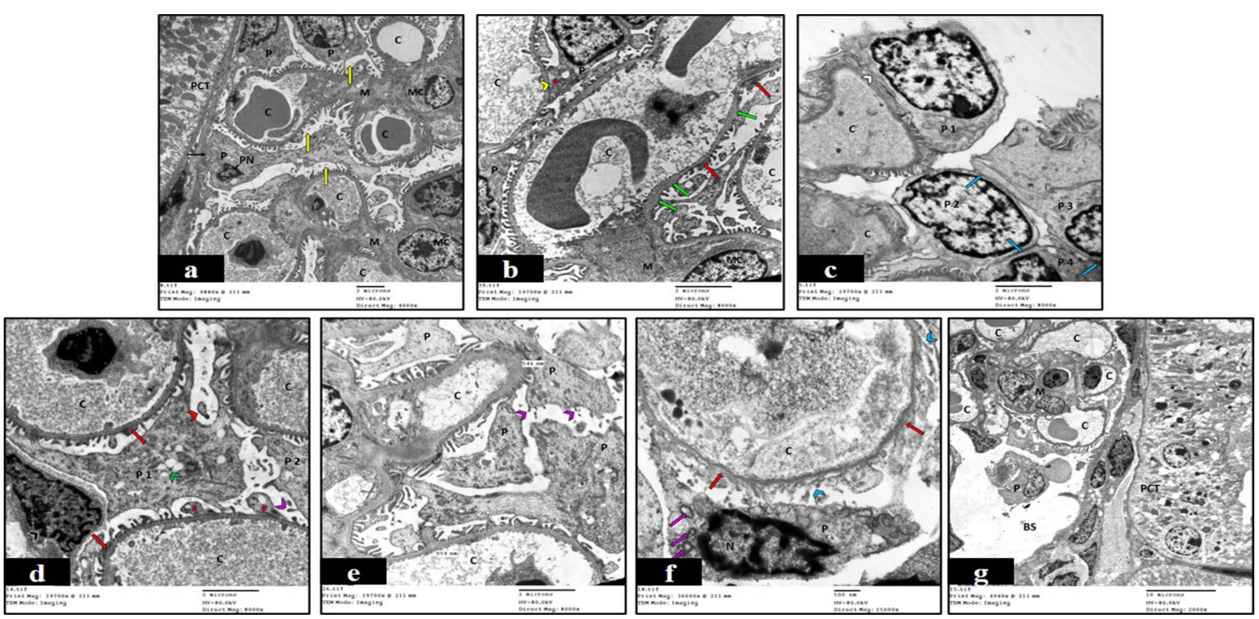

Fig. 5: Photomicrographs of the renal cortex from untreated unilateral nephrectomy group (group III):
[a]: parts of a glomerulus and a PCT (PCT). Podocytes (P) surround glomerular capillary loops (C). A close contact is noticed between the cell body of one podocyte -that has a pyknotic nucleus (PN)- and the parietal layer of Bowman's capsule (line arrow). The subpodocytic spaces are obviously wide (yellow arrows). Mesangial cells (MC) are surrounded by expanded mesangial matrix (M). [TEM, x4000]. [b]: glomerular capillary loops (C), podocytes (P), a mesangial cell (MC) with expanded matrix (M), and areas of GBM thickening are seen (green arrows). In some areas, foot processes are effaced (red arrows), while at another site they disappeared, and the major process (red dot) is covering the GBM directly (yellow arrow head). [TEM, x8000]. [c]: glomerular capillary loops (C) and 4 podocytes (P) are seen with adhesions (blue arrows) between podocytes 2,3&4. Part of the cell body of podocyte 1 can be seen directly covering the GBM (white arrow head). [TEM, x8000]. [d&e]: a parietal epithelial cell (black arrow head), podocytes (P) surrounded by glomerular capillary loops (C), and effaced foot processes (red arrows) are seen. Some major processes (red dots) are covering the GBM directly. Podocyte 1 shows multiple vacuolations (green arrow head), with an area of cytoplasm shedding (red arrow head). Microvillus transformation of podocytes (purple arrow heads) and localized areas of GBM thickening (where measurements are taken) can be seen. [TEM, x8000]. [f]: a glomerular capillary loop (C) and a podocyte (P) with heterochromatic nucleus (N) and endocytic vesicles (purple arrows) are shown. Foot processes appear distorted (blue arrow heads) with areas of effacement (red arrows). [TEM, x15000]. [g]: a PCT at the right side and a glomerulus at the left side with multiple glomerular capillary loops (C). A podocyte (P) can be seen floating in Bowman's space (BS). Mesangial expansion is noted (M) [TEM, x2000].

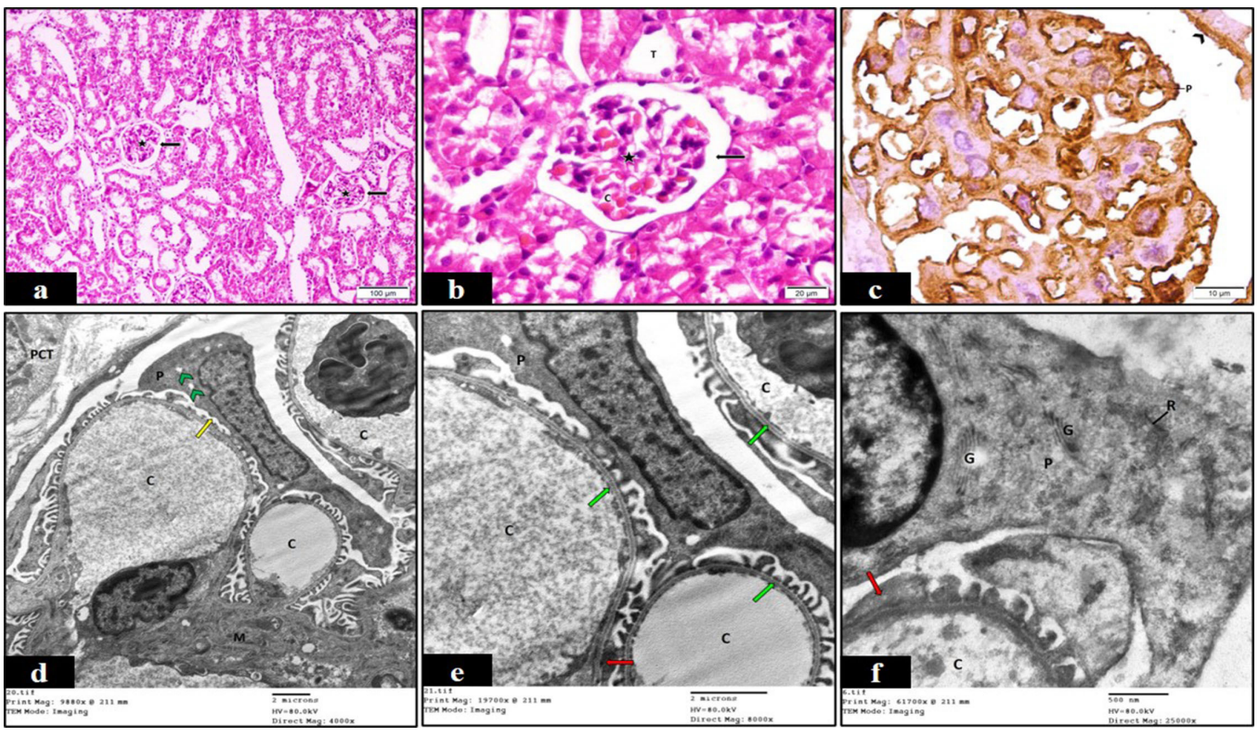

Fig. 6: Photomicrographs of the renal cortex from ACEI treated group (group IV):
[a&b]: normally appearing renal corpuscles surrounded by renal tubules (T). The glomerular tufts of capillaries (stars) are encircled by apparently normal Bowman's spaces (arrows). Glomerular capillaries show mild congestion and dilatation (C) [a: H&E, x100, b: H&E, x400]. [c]: weak positive cytoplasmic expression of nestin in podocytes (P) as well as the parietal layer of Bowman's capsule (arrow head) is detected. [anti nestin immunohistochemical stain, x1000]. [d&e]: showing a podocyte (P) with few small cytoplasmic vacuolations (green arrow heads), glomerular capillary loops (C), mesangial matrix (M) and Part of (PCT). The subpodocytic space is apparently normal (yellow arrow). GBM appears of a uniform thickness (green arrows). An area of effacement can be detected (red arrow). [d: TEM, x4000, e: TEM, x8000]. [f]: showing part of the cell body of a podocyte (P) and part of a glomerular capillary loop (C). The cytoplasm exhibits the presence of Golgi apparatus (G) and rER (R). A limited area of foot process effacement can be identified (red arrow). [TEM, x25000].

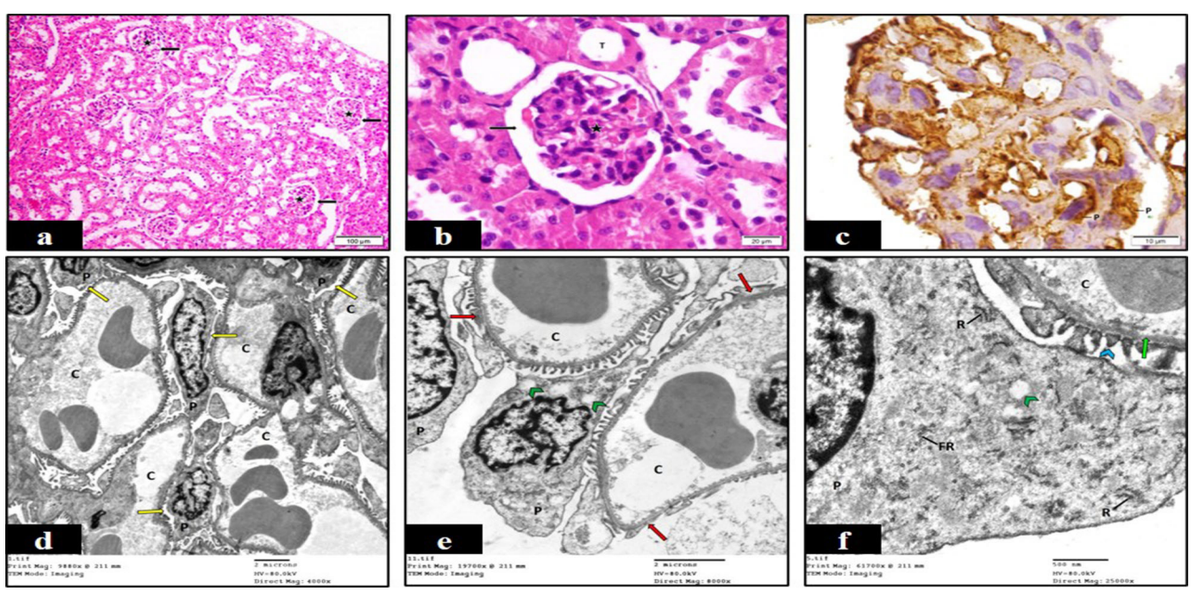

Fig. 7: Photomicrographs of the renal cortex from SGLT2I treated group (group V):
[a&b]: showing normally appearing renal corpuscles surrounded by renal tubules (T). The glomerular tufts of capillaries (stars) are encircled by seemingly normal Bowman's spaces (arrows) [a: H&E, x100, b: H&E, x400]. [c]: weak cytoplasmic expression of nestin in the podocytes (P). [anti nestin immunohistochemical stain, x1000]. [d&e]: showing podocytes (P) surrounding glomerular capillary loops (C). The subpodocytic spaces (yellow arrows) are apparently normal comparable to the control in Fig. (3d). Vacuolations within the cytoplasm of one podocyte can be detected (green arrow heads), in addition to foot process effacement (red arrows). [d: TEM, x4000, e: TEM, x8000]. [f]: showing a podocyte (P) and part of a glomerular capillary loop (C). rER can be visualized within the cytoplasm of the podocyte (R), free scattered ribosomes (FR) and few vacuolations are present (green arrow head). Foot processes (blue arrow head) with slit diaphragms in between are resting on a regular GBM (green arrow). [TEM, x25000].

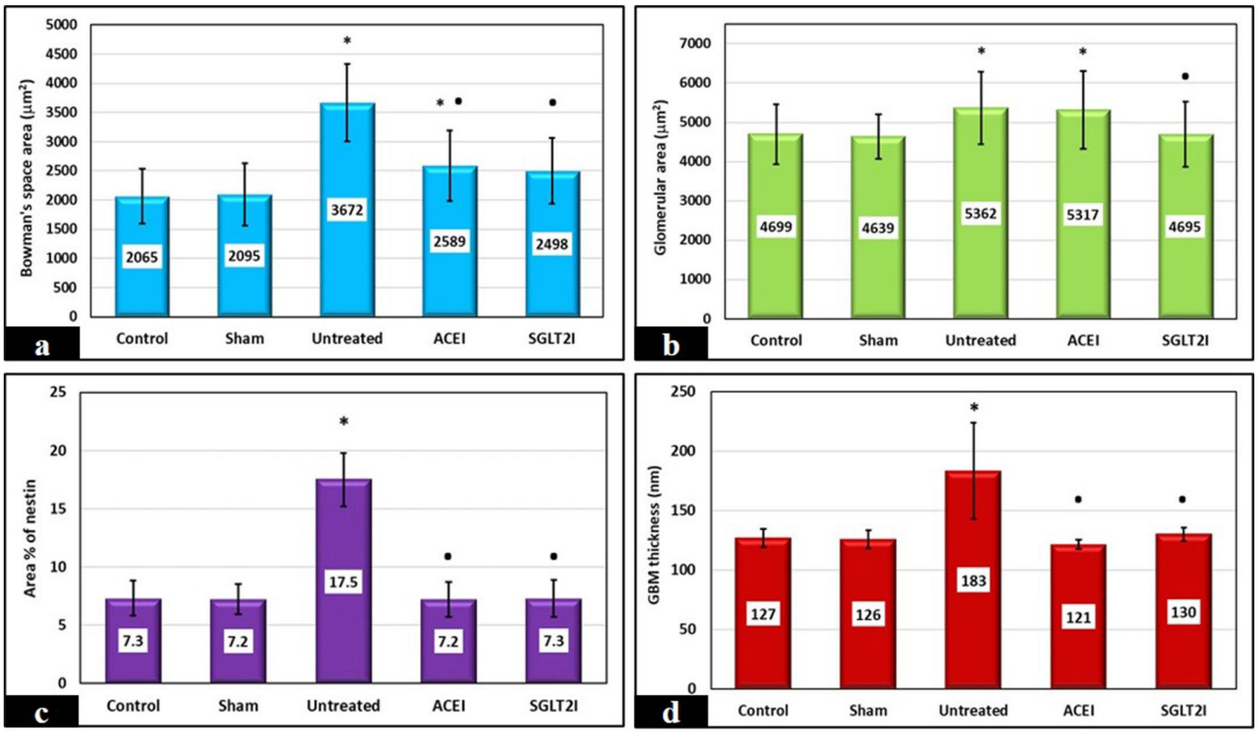

Fig. 8: Histograms showing [a]: Mean area of Bowman's space ± SD expressed in µm². *Significant increase as compared to control (*p-value* <0.05), •Significant reduction as compared to group III (*p-value* 0.05). [b]: Mean glomerular area ± SD expressed in µm². *Significant increase as compared to control (*p-value* <0.05), •Significant reduction as compared to group III (*p-value* <0.001). [c]: Mean area % ± SD of positive immune reaction of nestin. *Significant increase as compared to control (*p-value* <0.001), •Significant reduction as compared to group III (*p-value* <0.001). [d]: Mean GBM thickness ± SD expressed in nm. *Significant increase as compared to control (*p-value* <0.001), •Significant reduction as compared to group III (*p-value* <0.001).

DISCUSSION

Nephrectomy is a common surgical procedure that is not only performed in neoplastic renal conditions, but also in non-neoplastic ones[25], including unilateral nephrectomy in living kidney donation. Hence, the importance of scientific research in the field of renal mass reduction, targeting to find convenient treatments to mitigate the possible consequent maladaptive responses.

The current study aimed to detect the histological changes in podocytes following unilateral nephrectomy in young male albino rats, and to evaluate the possible ameliorative effect of SGLT2I versus ACEI by histological and morphometric studies. In this work, the ACEI was used as a reference drug (standard therapy for comparison), as it had been used in many previous studies and proved efficacy in similar models[11]. To achieve this aim, unilateral nephrectomy model in rodents was done for its well-known ability to induce hyperfiltration injury[3].

The study included young rats because the used drugs were targeting the glomerular capillary pressure, which increases early in the young but late in the adult following nephron loss. The most important in this model was to reduce the renal mass after the completion of nephrogenesis, which occurs at day 10 postpartum in rats[26].

All the groups -even the untreated one- showed no statistical difference in lab results for serum creatinine and 24-hour urinary albumin when compared to the control. Such results can be explained through some previous studies stating that the standard biomarkers of CKD including albuminuria occur at progressive stages of the disease. Therefore, advanced prognostic markers are needed to predict CKD risk early before the impairment of renal functions[27,28]. In addition, in most of the former studies done on non-diabetic rodents that detected albuminuria in CKD, the uninephrectomy was done to exaggerate another renal injurious factor[11]. Blood glucose level tests were not included in the current study, because SGLT2Is have minimal risk for hypoglycemia as they have counter-regulatory actions including insulin reduction and glucagon increase[29].

For all uninephrectomized rats (untreated and treated), the average weight of the remaining kidneys at time of sacrifice was significantly increased when compared to the control. According to a previous study[30], Compensatory renal hypertrophy (CRH) is the principal contributor to this growth. However, hyperplasia also occurs particularly in young animals.

Regarding the untreated uninephrectomized (group III) sections, most of the pathological changes that occurred at the H&E level could be attributed to secondary FSGS, which is encountered subsequent to significant nephron loss[31].

Hyalinosis occurrence was specified to be in the vascular pole area, just like the result of this study. However, it was detected in glomeruli not showing the manifestations of sclerosis, which could be explained by the presence of glomerular hypertension[32].

Glomerular distortion and adhesions were similarly encountered in a former study[33], which stated that early mesangial affection in FSGS results in ballooning of the glomerular capillaries, change in their arrangement, and consequently tuft distortion. This dislocation of capillaries brings podocytes in contact with the parietal epithelial cells and finally results in tuft adhesions and sclerosis.

The significant widening of Bowman's space area is an indicator of hyperfiltration (increased amount of primary urine in Bowman's space) and not a result of tuft shrinkage, as the glomerular area showed significant increase in group III sections when compared to the control.

Examination of immune-stained sections for nestin revealed positive normal diffuse nestin-stained cells in the control group. On the other hand, group III sections showed intense nestin expression with a significant increase in its area % when compared to the control. It was concluded that nestin (being an intermediate filament) plays an important role in the stability of podocytes, so they can respond to the tensile stress by morphological changes[18], which explains its intense expression in this group.

Ultrastructural examination of group III sections revealed many pathological changes that could also be attributed to secondary FSGS[32]. Podocytes have a unique way in responding to injury. Unlike other cells, they remain viable despite the marvelous shape changes they go through[34]. Moreover, podocytes have the ability to sense the mechanical stresses (like tensile stress and FFSS) and to react to them by mechanotransduction[35].

Vacuolization of podocytes is a pattern of their damage[36], which can be further explained by the reduction in their density consequent to their hypertrophy[37]. Another manifestation of cell material turnover is the shedding of cytoplasm[38].

The phenomenon of microvillus transformation had been described as a trial made by podocytes to search for attachment to GBM or parietal epithelial cells[32]. Recently, it was identified as one of the top ultrastructural predictors of prognosis in cases of podocytopathies[39]. It was found to be linked with an increased chance of remission and response to treatment[40].

In regards to the encountered effacement, foot processes become flatter and wider in response to injury[1]. It had been described that this effacement passes into several stages. It starts by displacement or disappearance of slit diaphragms with their replacement by occludens junctions, followed by retraction of the foot processes into the primary processes, and finally direct adherence of the podocyte's cell body to the GBM. The process of foot process effacement was also described as a survival strategy made by podocytes to increase their attachment to the GBM[41].

In the current work, foot process effacement showed localized distribution rather than a generalized pattern. Podocytes are mainly sensitive to FFSS[42], and since it is highest at the initial segment of the glomerular capillary and lowers toward the end (unequally distributed), therefore the process of effacement is heterogeneously distributed in cases of maladaptive FSGS[43].

Previous studies stated that immature podocytes connect to each other by tight junctions during early development, followed by widening of the intercellular spaces and slit diaphragm appearance. Meanwhile, tight junctions disappear and become no longer present in mature podocytes[44]. However, in the current study, adhesions could be detected between the cell bodies of podocytes which are apparently in the form of tight junctions. The first (and to our knowledge the only) one who reported the presence of tight junctions between neighboring podocytes by TEM was Succar and his colleagues, who identified them -in 2016- early in experimental crescentic glomerulonephritis[45]. Tight junctions between cell bodies of podocytes have never been mentioned as part of FSGS pathology. We believe the current study is the first to report such adhesions between the somas of non-detaching podocytes by TEM in a model of renal mass reduction. We suggest that these junctions were formed to resist the mechanical stresses to which podocytes were subjected, in an attempt to avoid detachment.

Finding detached viable podocytes is an expected consequence of the continuous exposure to mechanical stresses (high flows and shear stresses), leading to their separation from the GBM[37]. Several researchers suggested that in the majority of cases podocyte loss occurs by detachment as viable cells rather than by in situ necrosis or apoptosis[46,47]. However, we were able to detect chromatic condensation and pyknosis in some podocytes which are signs of podocyte damage[48].

The expansion of the subpodocytic space in many fields of this group could be explained by the excessive hypertrophy of podocytes resulting in cell body attenuation and consequently expansion of this space[49].

As for the GBM in group III sections, it showed significant increase in its thickness when compared to the control, even though the values of the mushroom like thickenings were not included in the statistical analysis. GBM thickening is a common histologic finding in cases of renal mass reduction[50]. A similar result of uneven irregular thickening of GBM was previously reported in a model of subtotal nephrectomy in Sprague- Dawley rats[51]. Studies done on diabetic nephropathy had clarified that the disturbance of the podocyte-GBM relation and the structural damage of podocytes are critical in the occurrence of GBM thickening[52,53].

Regarding ACEI treated uninephrectomized rats (group IV), kidney weight and glomerular area increased with insignificant difference when compared to the untreated rats (group III). Such result didn't come along with what

had been assumed that angiotensin II is by some means involved in glomerular hypertrophy which consequently can be inhibited by an ACEI[37]. However, our result went hand in hand with a recent study which proved that the chronic response of compensatory renal growth is independent of the RAAS[54].

The conservancy in the glomerular histoarchitecture in group IV sections was clear at the level of H&E, immunohistochemical staining, and TEM. This effect could be attributed to the ability of ACEIs and angiotensin receptor blockers (ARBs) to reduce glomerular capillary pressure, induce GBM remodeling, recover glomerular pore selectivity and decrease transforming growth factor beta (TGF-β), resulting in reduced mesangial proliferation[55]. These effects are opposing to the renin-angiotensin system effects[56]. It had been demonstrated by previous studies that treatment of sub-totally nephrectomized rats with a high dose of ACEI or ARB was effective in ameliorating glomerulosclerosis progression. On the other hand, it was documented that treatment with a single RAAS blocker is inadequate to promote long-lasting regression of glomerulosclerosis[57].

The remarkable effect obtained with the use of enalapril in the current work matched a previous one in which lisinopril (an ACEI) was used as a reference drug in mice subjected to protein-overload proteinuria on top of unilateral nephrectomy. It was reported that focal podocyte damage and areas of effacement were infrequent with the treatment.

Furthermore, similar to our finding, a significant reduction in nestin expression was proved in the ACEI treated rats[11]. The reduction in nestin expression points to an improvement in the cellular stress condition[18]. Since glomerular hypertension results in hyperfiltration[37], it can be concluded that reducing glomerular capillary pressure by an ACEI can indirectly reduce FFSS in addition to the direct control of tensile stress. This suggested reduction in hyperfiltration can also explain the narrowing of the subpodocytic spaces and the significant reduction in Bowman's space area in group IV when compared to the untreated group III. Lastly, GBM thickness in group IV didn't show any significant difference when compared to the control.

In regard to SGLT2I treated rats (group V), kidney weight and glomerular area were reduced when compared to group III. However, this reduction was not significant in kidney weight but significant in the glomerular area. These results partially agreed with what had been reported earlier, that ipragliflozin (an SGLT2I) neither helped with the renal hypertrophy nor reduced the glomerular area[9]. All the other parameters including Bowman's space area, glomerular area, area % of nestin, and GBM thickness showed significant reduction in group V sections when compared to the untreated rats (group III).

The reno protective effect of dapagliflozin was reflected on the renal histoarchitecture. This effect can be attributed to the drug's mechanism of action, which includes reduction of Na reabsorption in the proximal convoluted tubules, consequently increasing its delivery to the macula densa leading to a rise in adenosine triphosphate breakdown and adenosine production. Adenosine causes afferent arteriolar vasoconstriction resulting in reduction of glomerular capillary pressure and hyperfiltration[58].

All the parameters in group V rats did not show any significant difference when compared to ACEI treated rats (group IV). However, it could be noticed from the results of the current study that the ultrastructural changes in the ACEI treated rats were slightly better (less frequent vacuolations and effacement) than in dapagliflozin treated rats. The renoprotective effects of SGLT2Is could be further explained (in addition to their hemodynamic effects) by their ability to ameliorate renal hypoxia and fibrosis[59,60].

Regarding nestin expression by group V rats, the current study detected its significant reduction when compared to group III rats. This finding was similar to that of a previous study, that reported- in addition to nestin reduction- sodium glucose cotransporter 2 (SGLT2) expression on mice's podocytes, which increased during the stress of protein overload. Therefore, the authors made the conclusion that SGLT2Is have a direct effect on podocytes, and are able to affect their cytoskeletal rearrangement[11].

CONCLUSIONS

It could be concluded that the SGLT2I (dapagliflozin) can work on many levels to ameliorate the outcome by protecting against the maladaptive response following renal mass reduction, as it gave almost similar results to that of the ACEI. Thereby, using it as a protective drug in cases of solitary kidney following uninephrectomy would be of great benefit in controlling and delaying the process of glomerulosclerosis, especially in conditions in which RAAS blockers are contraindicated, untolerated, or inadequate.

ABBREVIATIONS

SGLT2I: Sodium–Glucose Cotransporter 2 Inhibitor, **ACEI:** Angiotensin Converting Enzyme Inhibitor, **TEM:** Transmission Electron Microscopy, **GBM:** Glomerular Basement Membrane, **FSGS:** Focal Segmental Glomerulosclerosis, **FFSS:** Fluid flow shear stress, **ESRD:** End Stage Renal Disease, **CKD:** Chronic Kidney Disease, **RAAS:** Renin- Angiotensin- Aldosterone System, **FDA:** Food and Drug Administration, **H&E:** Hematoxylin and Eosin, **PBS:** Phosphate Buffered Saline, **rER:** Rough Endoplasmic Reticulum, **CRH:** Compensatory renal hypertrophy, **ARB:** Angiotensin Receptor Blocker, **TGF-β:** Transforming Growth Factor Beta, **SGLT2:** Sodium–Glucose Cotransporter 2.

CONFLICT OF INTERESTS

There are no conflicts of interest.

REFERENCES

1. Garg P (2018). A Review of Podocyte Biology. Am. J. Nephrol. 47,3–13.
2. Butt L, Unnersjö-Jess D, Höhne M, Schermer B, Edwards A, Benzing T (2021). A mathematical estimation of the physical forces driving podocyte detachment, Kidney Int. 100(5):1054-62.
3. Srivastava T, Celsi GE, Sharma M, Dai H, McCarthy ET, Ruiz M, Cudmore PA, Alon US, Sharma R, Savin VA (2014). Fluid flow shear stress over podocytes is increased in the solitary kidney. Nephrol Dial Transplant. 29(1):65–72.
4. Maggiore U, Budde K, Heemann U, Maggiore U, Budde K, Heemann U, Hilbrands L, Oberbauer R, Oniscu GC, Pascual J, Schwartz Sorensen S, Viklicky O, Abramowicz D, & ERA-EDTA DESCARTES working group (2017). Long-term risks of kidney living donation: review and position paper by the ERA-EDTA DESCARTES working group. Nephrol Dial Transplant. 32(2):216–23.
5. Srivastava T, Hariharan S, Alon US, McCarthy ET, Sharma R, El-Meanawy A, Savin VJ, Sharma M (2018). Hyperfiltration-mediated injury in the remaining kidney of a transplant donor. Transplantation. 102(10):1624-35.
6. Haruhara K, Kanzaki G, Tsuboi N (2023). Nephrons, podocytes and chronic kidney disease: Strategic antihypertensive therapy for renoprotection. Hypertens Res 46(2):299–310.
7. Shiraishi T, Tamura Y, Taniguchi K, Higaki M, Ueda S, Shima T, Nagura M, Nakagawa T, Johnson RJ, Uchida S (2014). Combination of ACE inhibitor with nicorandil provides further protection in chronic kidney disease. Am J Physiol Renal Physiol. 307(12):1313–22.
8. Barrera-Chimal J, Lima-Posada I, Bakris GL, Jaisser F (2022). Mineralocorticoid receptor antagonists in diabetic kidney disease — mechanistic and therapeutic effects. Nat Rev Nephrol. 18(1):56–70.
9. Tanaka S, Sugiura Y, Saito H, Sugahara M, Higashijima Y, Yamaguchi J, Inagi R, Suematsu M, Nangaku M, Tanaka T (2018). Sodium–glucose cotransporter 2 inhibition normalizes glucose metabolism and suppresses oxidative stress in the kidneys of diabetic mice. Kidney International. 94(5):912–25.
10. Zhang Y, Nakano D, Guan Y, Hitomi H, Uemura A, Masaki T, Kobara H, Sugaya T, Nishiyama A (2018). A sodium-glucose cotransporter 2 inhibitor attenuates renal capillary injury and fibrosis by a vascular endothelial growth factor–dependent pathway after renal injury in mice. Kidney Int. 94(3):524–35.
11. Cassis P, Locatelli M, Cerullo D, Corna D, Buelli S, Zanchi C, Villa S, Morigi M, Remuzzi G, Benigni A, Zoja C (2018). SGLT2I dapagliflozin limits podocyte damage in proteinuric nondiabetic nephropathy. JCI Insight. 3(15): e98720.
12. Jafar TH (2021). FDA approval of dapagliflozin for chronic kidney disease: a remarkable achievement? Lancet. 398(10297):283-84.
13. US Food and Drug Administration. FDA approves treatment for chronic kidney disease. April 30, 2021 https://www.fda.gov/news-events/press announcements/fda-approves-treatment-chronic-kidney-disease.
14. Braunwald E (2022). SGLT2 inhibitors: the statins of the 21st century. Eur Heart J. 43(11):1029-30.
15. El-Kady MM, Naggar RA, Guimei M, Talaat IM, Shaker OG, Saber-Ayad M, Srivastava P, Pandey S (2021). Early Renoprotective Effect of Ruxolitinib in a Rat Model of Diabetic Nephropathy. Pharmaceuticals 14(7):608.
16. Khachatryan A, Tevosyan A, Novoselskiy D, Arakelyan G, Yushkevich A, Nazaretovich ND (2021). Rodents Anesthesia. Microsurgery Manual for Medical Students and Residents (1st ed). Springer. 111–14.
17. Kick BL, Gumber S, Wang H, Moore RH, Taylor DK (2019). Evaluation of 4 Presurgical Skin Preparation Methods in Mice. J Am Assoc Lab Anim Sci. 58(1):71–77.
18. Eladl MA, Elsaed WM, Atef H, El-Sherbiny M (2017). Ultrastructural changes and nestin expression accompanying compensatory renal growth after unilateral nephrectomy in adult rats. Int J Nephrol Renovasc Dis. 10:61–76.
19. Al-Qadhi G, Soliman M, Abou-Shady I, Rashed L (2020). Gingival mesenchymal stem cells as an alternative source to bone marrow mesenchymal stem cells in regeneration of bone defects: In *vivo* study, Tissue Cell. 63:101325.
20. Taha A, Khaled D, Ezz El Din M, Gouda M, El-Shafei A (2022). The Possible Protective Role of Verapamil and Dantrolene in Experimentally Induced Early Acute Pancreatitis in Male Albino Rat. Egyptian Journal of Histology. doi: 10.21608/ejh.2022.140968.1692.
21. Aguwa US, Nnamdi OS, Elizabeth EC, Janeth O, Nzube OB, Chukwuemeka OK, Ogbuokiri D, Chijioke O, Sopuru O, David O, Felix O (2020). Evaluating Methods of Rat Euthanasia on the Liver and Kidney of Wistar Rats: Cervical Dislocation, Chloroform Inhalation, Diethyl Ether Inhalation and Formalin Inhalation. Let Health BiolSci. 5(1):8-13.

22. Suvarna K, Layton C (2019). Bancroft J. The hematoxylins and eosin, Immunohistochemical techniques & Transmission electron microscopy. In Bancroft's Theory and Practice of Histological Techniques (8th ed). Elsevier. 126-38, 337-94, 434-75.

23. Ogorevc M, Kosovic I, Filipovic N, Bocina I, Juric M, Benzon B, Mardesic S, Vukojevic K, Saraga M, Kablar B, Saraga-Babic M. (2022). Differences in Immunohistochemical and Ultrastructural Features between Podocytes and Parietal Epithelial Cells (PECs) Are Observed in Developing, Healthy Postnatal, and Pathologically Changed Human Kidneys. Int J Mol Sci. 23(14):7501.

24. Viana DL, Alladagbin DJ, dos-Santos WLC, Figueira CP (2022). A comparative study of human glomerular basement membrane thickness using direct measurement and orthogonal intercept methods. BMC Nephrol. 23(1):23.

25. Kulkarni SP, Sonkawade D, Patro N, Kaur S, Sawadkar M (2019). Spectrum of lesions in non-neoplastic nephrectomy specimens and their clinico-pathological correlation-a tertiary care hospital experience. Indian J Pathol Oncol. 6(4):574-78.

26. Menendez-Castro C, Nitz D, Cordasic N, Jordan J, Bäuerle T, Fahlbusch FB, Rascher W, Hilgers KF, Hartner A (2018). Neonatal nephron loss during active nephrogenesis – detrimental impact with long-term renal consequences. Sci Rep. 8:4542.

27. Greenberg JH, Kakajiwala A, Parikh CR, Furth S (2018). Emerging biomarkers of chronic kidney disease in children. Pediatr. Nephrol. 33(6):925–33.

28. Bennett KM, Baldelomar EJ, Morozov D, Chevalier RL, Charlton JR (2021). New imaging tools to measure nephron number in *vivo*: opportunities for developmental nephrology. J Dev Orig Health Dis. 12(2):179-83.

29. Fattah H, Vallon V (2018). The potential role of SGLT2Is in the treatment of type 1 diabetes mellitus. Drugs.78(7):717-26.

30. Rojas-Canales DM, Li JY, Makuei L, Gleadle JM (2019). Compensatory renal hypertrophy following nephrectomy: When and how? Nephrology (Carlton). 24(12):1225-32.

31. Fogo AB, Kashgarian M (2017b). Diagnostic Atlas of Renal Pathology (3rd ed). Elsevier. Chapter 7 - Chronic Kidney Disease,457-62

32. Fogo AB, Kashgarian M (2017a). Diagnostic Atlas of Renal Pathology (3rd ed). Elsevier. Chapter 3 - Glomerular Diseases,19-294.

33. Kriz W, Wiech T, Gröne H (2022). Mesangial Injury and Capillary Ballooning Precede Podocyte Damage in Nephrosclerosis. Am J Pathol. 192(12):1670-82.

34. Kriz W, Shirato I, Nagata M, LeHir M, Lemley KV (2013). The podocyte's response to stress: the enigma of foot process effacement. Am J Physiol Renal Physiol. 304(4):333-47.

35. Endlich K, Kliewe F, Endlich N (2017). Stressed podocytes-mechanical forces, sensors, signaling and response. Pflugers Arch. 469(7-8):937–49.

36. Fogo AB, Cohen AH, Colvin RB, Jennette JC, Alpers CE (2014). Fundamentals of Renal Pathology (2nd ed). Springer Berlin, Heidelberg. 3-17.

37. Kriz W, Lemley KV (2015). A potential role for mechanical forces in the detachment of podocytes and the progression of CKD. J Am Soc Nephrol. 26(2):258-69.

38. Zeng L, Szeto C (2021). Urinary podocyte markers in kidney diseases. Clinica Chimica Acta. 523: 315-324.

39. Anders H-J, Boor P (2022). Predicting Future Outcomes from Kidney Biopsies with MCD/FSGS Lesions: Opportunities and Limitations. JASN 33(7):1233-35.

40. Zee J, Liu Q, Smith AR, Hodgin JB, Rosenberg A, Gillespie BW, Holzman LB, Barisoni L, Mariani LH (2022). Kidney Biopsy Features Most Predictive of Clinical Outcomes in the Spectrum of Minimal Change Disease and Focal Segmental Glomerulosclerosis. J Am Soc Nephrol. 33(7):1411-26.

41. Kriz W. (2020). The inability of podocytes to proliferate: cause, consequences, and origin. Anat. Rec. 303(10):2588–96.

42. Kriz W, Lemley KV (2017). Potential relevance of shear stress for slit diaphragm and podocyte function. Kidney Int. 91(6):1283–86.

43. Hommos MS, De Vriese AS, Alexander MP, Sethi S, Vaughan L, Zand L, Bharucha K, Lepori N, Rule AD, Fervenza FC (2017). The incidence of primary vs secondary focal segmental glomerulosclerosis: a clinicopathologic study. Mayo Clin. Proc. 92(12):1772–81.

44. Sun H, Li H, Yan J, Wang X, Xu M, Wang M, Fan B, Liu J, Lin N, Wang X, Li L, Zhao S, Gong Y (2022). Loss of CLDN5 in podocytes deregulates WIF1 to activate WNT signaling and contributes to kidney disease. Nat Commun. 13(1):1600.

45. Succar L, Boadle RA, Harris DC, Rangan GK (2016). Formation of tight junctions between neighboring podocytes is an early ultrastructural feature in experimental crescentic glomerulonephritis. Int J Nephrol Renovasc Dis. 24(9):297-312.

46. Bhathena DB (2003). Glomerular basement membrane length to podocyte ratio in human nephronopenia: implications for focal segmental glomerulosclerosis. Am J Kidney Dis. 41(6):1179-88.

47. Fukuda A, Chowdhury MA, Venkatareddy MP, Wang SQ, Nishizono R, Suzuki T, Wickman LT, Wiggins JE, Muchayi T, Fingar D, Shedden KA, Inoki K, Wiggins RC (2012). Growth-dependent podocyte failure causes glomerulosclerosis. J Am Soc Nephrol 23(3):1351–63.

48. Dong D, Fan Tt, Ji Ys, YU JY, WU S, Zhang L (2019). Spironolactone alleviates diabetic nephropathy through promoting autophagy in podocytes. Int Urol Nephrol 51(4):755–64.

49. Neal C, Crook H, Bell E, Harper S, Bates D (2005). Three-dimensional reconstruction of glomeruli by electron microscopy reveals a distinct restrictive urinary subpodocyte space. J Am Soc Nephrol. 16(5):1223–35.

50. Shim YW, Sol MY, Lee KM, Choi KU, Kim JY, Lee JS, Park DY, Lee CH, Suh KS (2002). Morphometric Analysis of Glomeruli in the Experimental Rat Models of Hyperglycemia and Hyperfiltration. Korean J Nephrol. 21(6):874-88.

51. Torras J, Herrero-Fresneda I, Gulias O, Flaquer M, Vidal A, Cruzado JM, Lloberas N, la Franquesa M, Grinyó JM (2009). Rapamycin has dual opposing effects on proteinuric experimental nephropathies: is it a matter of podocyte damage? Nephrol Dial Transplant. 24(12):3632–40.

52. Marshall SM (2007). The podocyte: A potential therapeutic target in diabetic nephropathy? Curr Pharm Des. 13(26):2713–20.

53. Marshall CB (2016). Rethinking glomerular basement membrane thickening in diabetic nephropathy: Adaptive or pathogenic? Am J Physiol Renal Physiol. 311(5):831–43.

54. Shimada S, Yang C, Kurth T, Cowley AW Jr (2022). Divergent roles of angiotensin II upon the immediate and sustained increases of renal blood flow following unilateral nephrectomy. Am J Physiol Renal Physiol. 322(5):473-85.

55. Sharma M, Singh V, Sharma R, Koul A, McCarthy ET, Savin VJ, Joshi T, Srivastava T (2022). Glomerular Biomechanical Stress and Lipid Mediators during Cellular Changes Leading to Chronic Kidney Disease. Biomedicines. 10(2):407.

56. Ruiz-Ortega M, Lamas S, Ortiz A (2022). Antifibrotic Agents for the Management of CKD: A Review. Am J Kidney Dis. 80(2):251-63.

57. Yang HC, Fogo AB (2014). Mechanisms of disease reversal in focal and segmental glomerulosclerosis. Adv Chronic Kidney Dis. 21(5):442–47.

58. Wanner C, Inzucchi SE, Lachin JM, Fitchett D, von Eynatten M, Mattheus M, Johansen OE, Woerle HJ, Broedl UC, Zinman B; EMPA-REG OUTCOME Investigators (2016). Empagliflozin and progression of kidney disease in type 2 diabetes. N Engl J Med. 375(4):323-34.

59. Zhao Y, Xu L, Tian D, Xia P, Zheng H, Wang L, Chen L (2018). Effects of sodium-glucose co-transporter 2 (SGLT2) inhibitors on serum uric acid level: a meta-analysis of randomized controlled trials. Diabetes Obes. Metab. 20(2):458–62.

60. DeFronzo RA, Reeves WB, Awad AS (2021). Pathophysiology of diabetic kidney disease: impact of SGLT2Is. Nat. Rev. Nephrol. 17(5):319–34.

الملخص العربى

التقييم الهستولوجي للتأثير المحسّن المحتمل لمثبط SGLT2 مقابل مثبط ACE علي الخلايا القدمية بعد استئصال الكلية من جانب واحد في صغار ذكور الجرذان البيضاء

مريم عزت حلمي، داليا فتحي الديب، إيمان عباس فرج، سامية حمدي رضوان

قسم علم الأنسجة، كلية الطب، جامعة القاهرة، القاهرة، مصر

الهدف من البحث: هَدَفَ هذا العمل الي كشف التغيرات الهستولوجية التي تحدث في الخلايا القدمية بعد إستئصال إحدى الكليتين في صغار ذكور الجرذان البيضاء، ولتقييم التأثير المحسّن المحتمل لمثبط SGLT٢ ومقارنته بمثبط ACE كدواء مرجعي، وذلك عن طريق دراسات هستولوجية وقياسية.

مواد وطرق البحث: شملت هذه الدراسة ثمانية وأربعين من ذكور الجرذان البيضاء في عمر شهر (~٥٠- ٦٠جم)، تم تقسيمهم كالتالي: المجموعة الأولى (المجموعة الضابطة): تم إعطاء ستة جرذان ٠,٥مل ماء مقطر عن طريق أنبوبة معدية مرة يومياً إلي وقت التضحية. المجموعة الثانية (المجموعة ذات العملية الزائفة): تعرض ستة جرذان لعملية زائفة عن طريق التلاعب بالكُلية اليسرى بدون ربط الأوعية الكُلوية أو الحالب. وتم إعطاؤهم ٠,٥مل ماء مقطر عن طريق أنبوبة معدية مرة يومياً إلي وقت التضحية. المجموعة الثالثة (مجموعة الإستئصال الغير معالجة): تم إعطاء إثنى عشر من الجرذان المستئصلة كُليتهم من جانب واحد ٠,٥مل ماء مقطر عن طريق أنبوبة معدية مرة يومياً إلي وقت التضحية. المجموعة الرابعة (المجموعة المعالجة بمثبط ACE): تم إعطاء إثنى عشر من الجرذان المستئصلة كُليتهم من جانب واحد إيزابريل عن طريق أنبوبة معدية مرة يومياً من بعد العملية وإلي وقت التضحية، بجرعة ١٠ملجم/كجم/يوم. المجموعة الخامسة (المجموعة المعالجة بمثبط SGLT٢): تم إعطاء إثنى عشر من الجرذان المستئصلة كُليتهم من جانب واحد فوركسيجا عن طريق أنبوبة معدية مرة يومياً من بعد العملية وإلي وقت التضحية، بجرعة ١,٥ملجم/كجم/يوم. تم تجميع عينات دم وبول من جميع الجرذان قبل التضحية، وكل جرذ خضع لقياس نسبة الكرياتينين في السيروم ونسبة الألبيومين في البول المجمع خلال ٢٤ ساعة. تم التضحية بجميع الجرذان عن طريق الخلع العنقي بعد مرور إسبوعين من العملية الزائفة وعملية الإستئصال، أعقبها إستخراج كُلاهم اليمنى (المتبقية). تم حفظ بعض أجزاء من الكُلي اليمنى في ١٠٪ محلول الفورمول المتعادل، وتجفيفها في تركيزات متصاعدة من الإيثانول، ثم غمرها في البارافين. تم تقطيع العينات وتعريضها للآتي: ١-صبغة الهيماتوكسلين و الإيوسين للتقييم الهستولوجي. ٢-الصبغة الهستوكيميائية المناعية للخيط المتوسط نيستين. تم حفظ كتل حوالي ٣ مم ٣ من النسيج القشري للكُلى اليمني بالغمر في ٢,٥ ٪ جلوترالدهايد في محلول الفوسفات المتعادل (٠,١ مول/ل، أس هيدروجيني ٧,٢)،ثم أضيفت الي مثبت آخر وهو ١ ٪ رباعي أكسيد الأوزميوم في محلول الفوسفات المتعادل (٠,١ مول/ل، أس هيدروجيني ٧,٢)، ثم تجفيفها في تركيزات متصاعدة من الإيثانول،و غمرها في مادة صمغية، ثم بلمرتها عند٦٠° سيليزية. تم تقطيع القوالب الصمغية بسُمْك ٦٠ نانومتر بواسطة سكين زجاجي. تم وضع المقاطع الرفيعة للغاية على شبكات نحاس عارية ثم صبغها بخلات اليورانيل وسترات الرصاص، وتم فحصها بواسطة المجهر الإلكتروني النافذ بتكبيرات مختلفة، كما تم قياس سُمْك الغشاء القاعدي للكبيبات الكُلوية. الدراسة المترية الشكلية: بإستخدام برنامج تحليل الصورة الضوئي، تم قياس المتغيرات

الآتية: ● مساحة محفظة بومان. ● مساحة الكبيبات الكُلوية. ● النسبة المئوية لمساحة التفاعل المناعي للنيستين. التحليل الإحصائي: بإستخدام تحليل التباين الإحصائي الأحادى، ثم بعد ذلك إختبار توكي للمقارنات البعدية المزدوجة.

نتائج البحث: أظهرت نتائج هذه الدراسة الآتي: أظهر جرذان المجموعتين الضابطة وذات العملية الزائفة تركيب نسيجي طبيعي بدون أي إختلاف في الدلالات الإحصائية بينهم في كل الدراسات القياسية التي تم عملها. أظهرت جميع الجرذان المستئصلة كُلاهم من ناحية واحدة (المعالجين والغير معالجين) زيادة ذات دلالة إحصائية في وزن الكُلية المتبقية كنتيجة للتضخم التعويضي وذلك عند مقارنتهم بالمجموعة الضابطة. وبالرغم من ذلك، هذه المجموعات لم تظهر أي إختلاف ذو دلالة إحصائية في نتائج التحاليل التي تم عملها عند مقارنتهم بالمجموعة الضابطة. أظهرت الجرذان المستئصلة كُلاهم من ناحية واحدة الغير معالجين (المجموعة الثالثة) الملامح الكلاسيكية لتصلب الكبب الكُلوية الجزئي البؤري في القطاعات المصبوغة بالهيماتوكسلين والإيوسين، والمصبوغة بالصبغة الهستوكيميائية المناعية للنيستين، والتي تم فحصها بواسطة المجهر الإلكتروني النافذ، بوجود تشوه شديد في التركيب الطبيعي للنسيج. جميع القياسات التي تمت لهذه المجموعة، والتي شملت مساحة محفظة بومان، مساحة الكبيبات الكُلوية، النسبة المئوية لمساحة التفاعل المناعي للنيستين، و سُمْك الغشاء القاعدي للكبيبات الكُلوية أظهرت زيادات ذات دلالة إحصائية عند مقارنتهم بالمجموعة الضابطة. أظهرت الجرذان المعالجة بعد إستئصال كُليتهم من جانب واحد (المجموعتان الرابعة والخامسة) وفيات (جرذ من المجموعة الرابعة واثنين من الخامسة). ومع ذلك، أظهرت الجرذان الحية درجة كبيرة من الإحتفاظ بالتركيب النسيجي للكبيبات الكُلوية، مع الحد الأدنى للتشوهات، حيث أن طمس الزوائد القدمية والفراغات في الخلايا القدمية نادراً ما واجهناهم. كلا المجموعتين أظهرا نقص ذو دلالة إحصائية في مساحة محفظة بومان، النسبة المئوية لمساحة التفاعل المناعي للنيستين، و سُمْك الغشاء القاعدي للكبيبات الكُلوية، وذلك عند مقارنتهم بالمجموعة الثالثة. ومع ذلك، لم يوجد أي إختلاف ذو دلالة إحصائية ما بين المجموعتين، مما يدل على تأثيرهم المتشابه تقريباً.

الإستنتاج:

- التناول المبكر لعقار الداباجليفلوزين بعد إنقاص كتلة الكُلية يُحَسّن من النتيجة ويحمي من الآثار الضارة لآلية التكيّف التعويضي.
- داباجليفلوزين مؤثر بدرجة متساوية تقريباً مع مثبط ال ACE (إنالابريل) في هذا النموذج من إستئصال الكُلية من جانب واحد.
- يمكن إعطاء الداباجليفلوزين في حالات الفشل الكُلوى المزمن الغير مُصَاحَب بمرض السكر حينما يكون مثبط ال ACE ممنوع أو غير كافي.